

Experimental Validation of the KC Autotuner on a Highly Nonlinear Vertical Take-Off and Landing (VTOL) Process

Robin De Keyser¹, Isabela R. Birs², and Cristina I. Muresan²

¹DySC Research Group on Dynamical Systems and Control, Ghent University, Ghent, Belgium

²Automation Department, Technical University of Cluj-Napoca, Cluj-Napoca, Romania

Email: Robain.DeKeyser@ugent.be; {Isabela.Birs; Cristina.Muresan}@aut.utcluj.ro

Abstract—The paper focuses on a novel PID (proportional integral derivative) autotuner based on a single experimental sine test. The Kiss Circle (KC) autotuner design and validation are targeted on a vertical take-off and landing platform which exhibits a highly oscillatory non-linear motion with time delay. An additional autotuner fit for time delay processes such as the well-known Ziegler-Nichols method is used to determine a PID controller for the Vertical Take-Off and Landing (VTOL) process. The experimental results obtained with the two different experimental tuning methods under several operating conditions are compared, illustrating the superiority of the KC autotuner.

Index Terms—KC autotuner, PID control, PID autotuning, nonlinear process

I. INTRODUCTION

In 1984, an initial version of the autotuner concept was introduced by Astrom and Hagglund [1] with the purpose of facilitating the process of computing proportional integral derivative (PID) parameters through minimum effort. The purpose was to create a self-tuned controller which can be easily used by persons who lack complex control engineering knowledge [2].

Among the years, many works such as [3]-[7] contributed to the development of the autotuner concept transforming it into a reliable tool in controller tuning. The usability of autotuners spans from simple processes such as the ones presented in [8] to more complex industrial processes, like sheet metal forming [9], nonlinear processes [10], or second order unstable loops [11]. The “self tuned” PID controllers should be mindful of closed loop stability and fulfillment of multiple tuning requirements.

The majority of available autotuning techniques are based on process response when fed a sinusoidal input. The sine wave frequency is determined through a relay test. Methods such as the popular Ziegler-Nichols (ZN) seek a critical frequency where the phase shift is -180° . The approach towards determining the PID parameters

lays in using data read from the sinusoidal response of the process and computing the parameters based on provided mathematical formulas [12]-[15].

This paper presents a novel PID tuning procedure named the KC (Kiss Circle) autotuner [16]. A fractional order extension of the KC method has been published in [5]. The method is based on a single sine test applied as the process input from which the parameters of the controller are computed. A forbidden region is defined on the Nyquist diagram that includes the -1 point. The computed PID controller is validated experimentally on a Vertical Take-Off and Landing (VTOL) platform. Performances such as settling time, overshoot, and robustness are assessed and the method proves useful in reference tracking and disturbance rejection.

Additional validations are realized by comparing the KC autotuner to the popular ZN method. The PID controllers are compared for several working areas of the process and also for disturbance rejection capabilities. The experimental tests prove the superiority of the KC autotuner procedure over the ZN method. Further comparisons regarding the ZN autotuner method were presented in [17].

The structure of the paper is organized as follows. The mathematical background of the KC autotuner is provided in Section II with all the necessary formulas needed for tuning the PID controller. Section III presents the description of the VTOL process as well as experimental data to show the nonlinear complexity of the process. The PID controllers are tuned using the KC and ZN methods in Section IV, whereas the experimental results gathered from the VTOL process are shown in Section V. Finally, Section VI concludes the paper.

II. MATEHMATICAL BACKGROUND OF THE KC AUTOTUNER

The transfer function of a PID controller can be defined by

$$C(s) = k_p \left(1 + \frac{1}{T_i s} + T_d s \right) \quad (1)$$

with k_p being the proportional gain, T_i and T_d the integral and derivative time constants. In the KC autotuning approach, the three parameters denoting the PID

Manuscript received April 30, 2019; revised June 28 2019; accepted August 5, 2019.

Corresponding author: Isabela R. Birs (email: isabela.birs@aut.utcluj.ro)

controller are computed in the absence of a process model, using the value of the process frequency response and the slope of the frequency response at a given frequency denoted by $\bar{\omega}$. The frequency data can be acquired experimentally by exciting the plant with a sine wave of frequency $\bar{\omega}$ and interpreting the output sinusoidal movement.

The first step in the KC autotuner algorithm is to define a forbidden region in the Nyquist plane which encloses the -1 point. The defined forbidden region is depicted in Fig. 1 with red, while the open loop frequency response is drawn with blue. The two points A and B on the Nyquist plot define the minimum gain and phase margins. The chosen constraints for the tuning are defined as the gain margin, $GM=2$, and the phase margin, $PM=45^\circ$.

Let us consider the loop frequency response which can be defined as

$$L(j\omega) = P(j\omega)C(j\omega) \quad (2)$$

The derivative of the loop frequency response can be written as a sum of its real and imaginary parts.

$$\frac{dL(j\omega)}{d\omega} \Big|_{\omega=\bar{\omega}} = \frac{dR_L(j\omega)}{d\omega} \Big|_{\omega=\bar{\omega}} + j \frac{dI_L(j\omega)}{d\omega} \Big|_{\omega=\bar{\omega}} \quad (3)$$

The interest falls upon the slope of $L(j\omega)$ which can be computed using the ratio $dI_L/dR_L|_{\omega=\bar{\omega}}$.

A point on the KC circle in Fig. 1 can be defined by using trigonometry as

$$\text{Re}(\alpha) = -C + R \cos \alpha, \quad \text{Im}(\alpha) = -R \sin \alpha \quad (4)$$

Leading to the border of the slope of the forbidden region:

$$\frac{d \text{Im}}{d \text{Re}} \Big|_{\alpha} = - \frac{\text{Re}(\alpha) + C}{\text{Im}(\alpha)} = \frac{\cos \alpha}{\sin \alpha} \quad (5)$$

From the Nyquist plot in Fig. 1 the slope of the forbidden region border can be defined as the ratio between the derivative of the imaginary and real parts as a function of the angle α . Hence, the slope is defined by $d \text{Im}/d \text{Re}|_{\alpha}$. The open loop frequency response is defined in a similar manner by $dI_L/dR_L|_{\omega=\bar{\omega}}$. The actual tuning of the PID controller becomes an optimization problem where the difference between the two slopes should be minimum. In order to determine the three parameters needed for the PID control law, one must solve the following equation:

$$\min_{\alpha} \frac{d \text{Im}}{d \text{Re}} \Big|_{\alpha} - \frac{dI_L}{dR_L} \Big|_{\bar{\omega}}, \quad 0 \leq \alpha \leq 90^\circ \quad (6)$$

A solution to solve the minimization problem is to take α in small increments of 1° starting from 0 to 90° .

The slope of the loop frequency response can be defined as the derivative of the loop frequency response:

$$\frac{dL(j\omega)}{d\omega} \Big|_{\omega=\bar{\omega}} = P(j\bar{\omega}) \frac{dC(j\omega)}{d\omega} \Big|_{\omega=\bar{\omega}} + C(j\bar{\omega}) \frac{dP(j\omega)}{d\omega} \Big|_{\omega=\bar{\omega}} \quad (7)$$

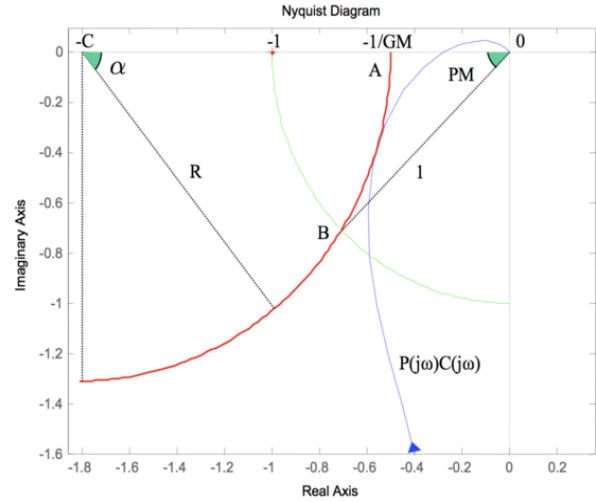


Fig. 1. Nyquist forbidden region (red) and open loop frequency response (blue).

In order to obtain $P(j\bar{\omega})$ one must excite the process by a sine wave of frequency $\bar{\omega}$. The same test is used to compute $dP(j\omega)/d\omega|_{\omega=\bar{\omega}}$ as shown in [16] and [18].

Knowing the desired loop frequency response as well as the process frequency response, the controller's transfer function can be written as

$$C(j\bar{\omega}) = \frac{L(j\bar{\omega})}{P(j\bar{\omega})} = \alpha \left(1 + j \frac{b}{a} \right) \quad (8)$$

Equations (1) and (8) both express transfer functions of the PID controller denoted by $C(s)$. Mapping the Laplace domain into the frequency domain is realized using $s = j\bar{\omega}$.

Writing the equality:

$$k_p \left(1 + \frac{1}{T_i j\bar{\omega}} + T_d j\bar{\omega} \right) = \alpha \left(1 + j \frac{b}{a} \right)$$

gives the proportional gain as

$$k_p = \alpha \quad (9)$$

Furthermore, the derivative time T_d is chosen as

$$T_d = \frac{T_i}{4} \quad (10)$$

Replacing (10) and $1/j = -j$ in $1/(T_i j\bar{\omega}) + T_d j\bar{\omega} = jb/a$ gives the second order equation:

$$T_i^2 \bar{\omega}^2 a - 4T_i \bar{\omega} b - 4a = 0$$

The equation is solved by using $\Delta = 16\bar{\omega}^2 (b^2 + a^2)$ and T_i is obtained as

$$T_i = \frac{4\bar{\omega} b \pm 4\bar{\omega} \sqrt{b^2 + a^2}}{\bar{\omega}^2 a}$$

Only the positive value is appropriate for the PID controller giving

$$T_i = \frac{2}{a\bar{\omega}} \left(b + \sqrt{b^2 + a^2} \right) \quad (11)$$

III. THE VTOL PROCESS

A. Description

The VTOL experimental platform depicted in Fig. 2 is designed by National Instruments and is compatible with real-life microcontrollers such as the NI Elvis. Graphical programming languages such as LabVIEW are used to communicate to the NI Elvis for real-time data acquisition and motion control. LabVIEW features an integrated control design add-on allowing the usage of real-time control loops in the Laplace domain. Hence, controllers can be directly implemented without the need of discretization.



Fig. 2. Vertical VTOL platform from national instruments.

The platform houses a cantilever beam equipped with a fan enclosed by safety guards to the right and a balancing weight to the left. The beam is fixed at one point along the length of cantilever at 1/3 near the weight. The setup has the possibility to rotate around the fixed point in the interval $[-26^\circ, 60^\circ]$.

The input of the process is the voltage applied to the DC motor actuating upon the fan, while the output is considered the angular displacement of the beam around the fixed point. The angular displacement is measured with respect to the fixed point; the 0 degree position is obtained when the beam is parallel to the base of the platform.

B. Plant Nonlinearity and SOPDT Model

The process is highly nonlinear due to the angular movement of the fan/weight. The initial position of the VTOL platform in the lack of any input signal is at -26° . In order to bring the platform in the 0 position a voltage input of 6.3 V is necessary.

Experimental tests have been performed with the purpose of linearity analysis by exciting the platform with different step input voltages. The experiments are performed after the platform is brought to the horizontal position. The test implies exciting the process with a 6.3 V input in order to reach the 0 position. Furthermore, step variations of -1.5 V and $+1.5$ V are applied, hence the input varies between 4.8 V and 7.8 V. The results are presented in Fig. 3. The figure shows the angular displacement of the beam with blue and the normalized values around 6.3 V of the input signal with black. As can be observed, the physical nature of the process response is different around the chosen operating conditions. Two more identical tests have been performed and the results show the same nonlinearity features as the ones presented in Fig. 3.

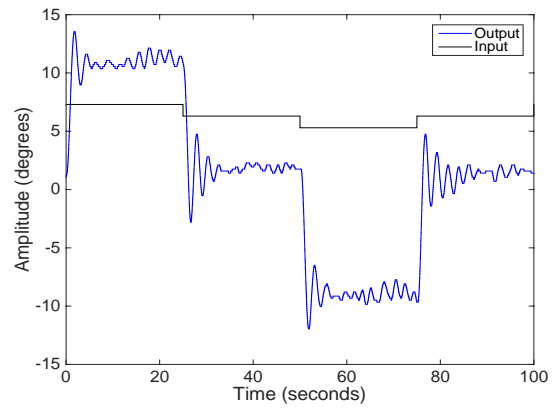


Fig. 3. Step experimental test.

A second order plus dead time (SOPDT) model is identified based on the experimental data. The model is not used to tune the PID controller using the previously presented KC method. However, this model will be further used to validate the test frequencies for the KC and ZN methods.

The four step responses are normalized and their values are averaged in Fig. 4. It is clear that the model is a high order complex transfer function. However, in order to use experimental tuning methods, the process is approximated to a second order plus dead time (SOPDT) transfer function

$$P(s) = \frac{10e^{-0.27s}}{0.20s^2 + 0.19s + 1} \quad (12)$$

The validation of the SOPDT model is shown in Fig. 5.

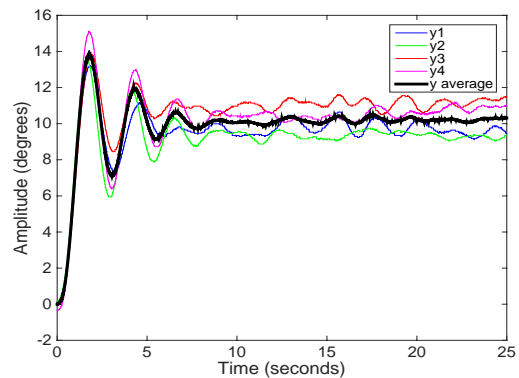


Fig. 4. Average of the step experimental test.

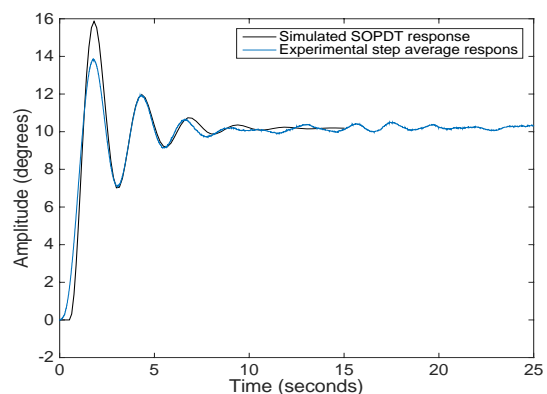


Fig. 5. SOPDT model and experimental averaged data.

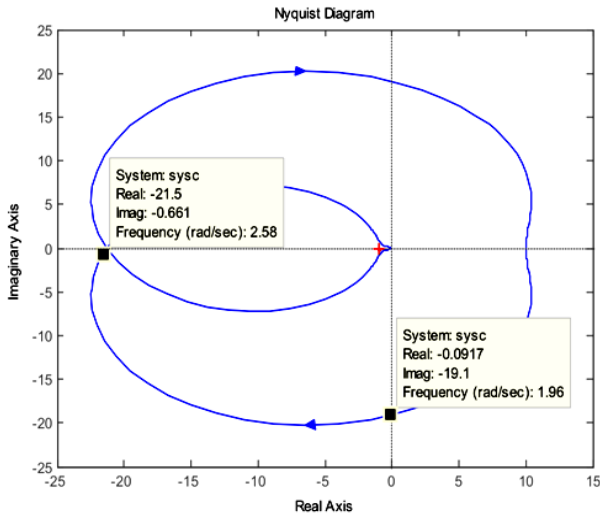


Fig. 6. Nyquist plot of the SOPDT model.

IV. CONTROLLER TUNING

Two PID controllers are tuned for the VTOL platform with the purpose of reference tracking, improved settling time and reduced overshoot. The main controller is the one tuned through the KC method presented throughout the paper. An additional controller is tuned using the popular ZN for method validation and comparison purposes.

The choice of the ZN method for comparison is justified by the similarities between the two methods: both tuning procedures are based on experimental sinusoidal response and both methodologies require a test frequency to perform the sine tests.

The test frequency required by the KC tuner is located around the magnitude peak, where the phase $\varphi = -90^\circ$. In the ZN scenario, the test frequency is the critical frequency where $\varphi = -180^\circ$. The two frequencies can be determined from the Nyquist plot (Fig. 6) of the previously identified SOPDT model.

In absence of a SOPDT model, both frequencies can be determined experimentally via a relay test.

A. KC Controller Tuning

The experimental setup is fed with a sine wave of frequency $\omega=2$ rad/s and normalized amplitude of 0.5 V.

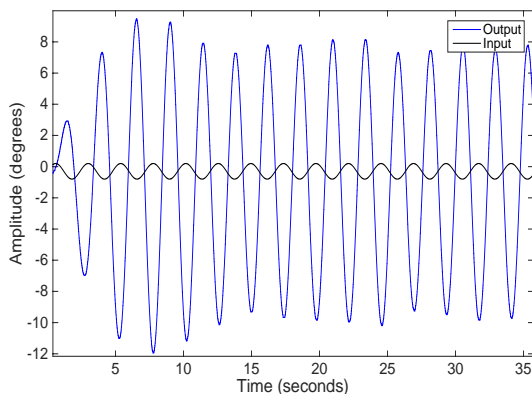


Fig. 7. Average of VTOL output for three identical sinusoidal inputs with frequency $\omega = 2$ rad/s.

The initial conditions are similar to the ones presented in the step experiments: input of 6.3 V and 0 angular displacement. Three identical consecutive tests are performed and the process output is averaged in Fig. 7. The averaged sine wave values are used to compute the PID controller using the KC tuning procedure.

The process value at the test frequency $\omega = \bar{\omega} = 2$ rad/s is determined as

$$P(j\bar{\omega}) = 3.38 - 18.4j = 18.7e^{-1.38j} \quad (13)$$

while the derivative of the frequency response needed to solve (7) is obtained as

$$\left. \frac{dP(j\omega)}{d\omega} \right|_{\omega=\bar{\omega}} = -90.2 + 1.25j \quad (14)$$

The parameters of the PID controller are obtained from (9), (10), (11) as $k_p = 0.00114$, $T_i = 0.0206$ and $T_d = 0.00515$ and the controller from (1) can be written as

$$C(s) = 0.00114 \left(1 + \frac{1}{0.0206s} + 0.00515s \right) \quad (15)$$

B. ZN Controller Tuning

ZN is one of the most popular experimental tuning approaches due to its practicality and systematic tuning of the controller. The method is based on experimental process response to an input consisting of a sinusoidal signal with the frequency equal to the system's critical frequency. The critical frequency can be graphically interpreted as a phase shift of -180° . These particular frequency domain rules have been applied on physical processes [19].

The first step in the ZN algorithm is to determine the process' critical frequency. The Nichols plot from Fig. 6 as well as experimental relay tests identify the critical frequency as $\omega_{cr} = 2.56$ rad/s.

For the VTOL process, three identical sine tests have been performed with an input of amplitude 1 V and frequency $\omega=2.56$ rad/s. The averaged values of the three tests are shown in Fig. 8.

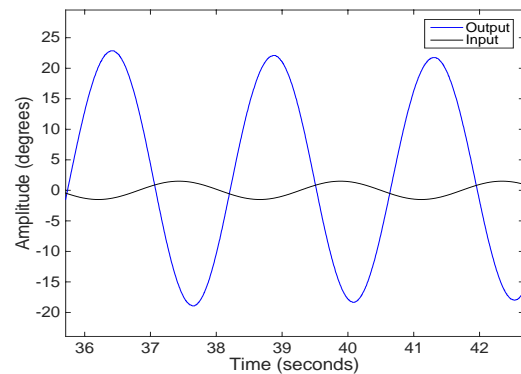


Fig. 8. Average of VTOL output for three identical sinusoidal inputs with frequency $\omega = 2.56$ rad/s.

The average signal is a sine wave having the same critical frequency as the input and an amplitude of 19° . The critical gain can be determined from the ZN tuning rules as

$$k_c = \frac{1}{19} = 0.0526 \quad (16)$$

while the period of oscillation is computed as

$$T = 2\pi/\omega = 2.45s \quad (17)$$

Furthermore, the PID parameters are determined from

$$k_p = 0.6K_c = 0.03 \quad (18)$$

$$T_i = 0.5T = 1.225 \quad (19)$$

$$T_d = 0.125T = 0.306 \quad (20)$$

resulting the following ZN controller:

$$C_{ZN}(s) = 0.03 \left(1 + \frac{1}{1.225s} + 0.306s \right) \quad (21)$$

V. EXPERIMENTAL RESULTS AND COMPARISON

The two PID controllers from (15) and (21) are validated through experimental tests that focus on reference tracking performance as well as input disturbance rejection.

The first test gives a step change of the reference signal between 0° and 10° . The controllers were tuned based on this operating point. The experimental VTOL results for the closed loop system with the KC and ZN controllers are presented in Fig. 9.

The initial conditions for the VTOL process are angular position of 0° and command signal of 6.3 V. At $t=10$ s a step reference from 0° to 10° is given. As can be seen in Fig. 9 the closed loop system successfully follows the reference signal for both controllers. However, the settling time obtained with the KC controller is $t_{sKC} = 5$ s, which is 10 s faster than the settling time obtained with the ZN controller $t_{sZN} = 15$ s. Also, both controllers give a 0° overshoot. Another step reference from 10° to 0° is given at $t=35$ s. For this step choice, the settling time exhibited by the closed loop process with the KC controller is $t_{sKC}=8$ s compared to the $t_{sZN}=20$ s obtained with the ZN method.

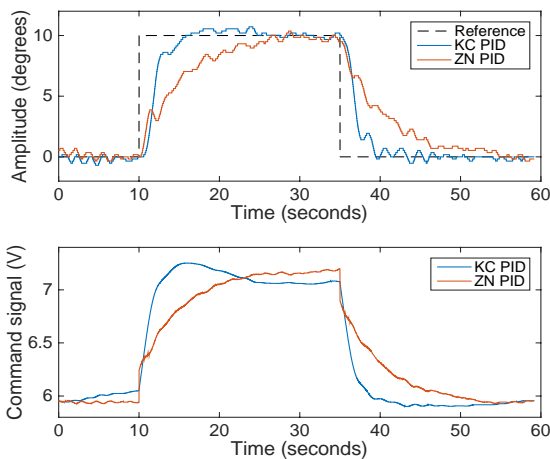


Fig. 9. Experimental closed loop system response with ZN and KC controllers.

The presented experimental test proves that the KC controller is a better choice than the ZN for reference tracking purposes. For a deeper analysis, the disturbance rejection performance is also analyzed. A step disturbance of amplitude 1 V that acts upon the command signal is introduced into the system. The results regarding beam displacement can be seen in Fig. 10.

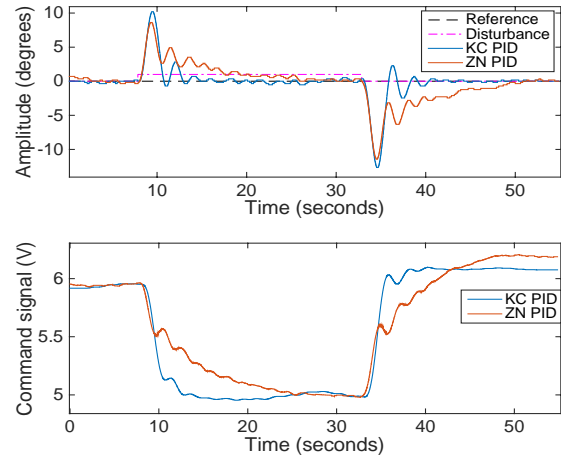


Fig. 10. Experimental disturbance rejection.

The system's initial condition is identical to the reference tracking experiment. At time $t=8$ s, a 1 V disturbance is injected into the command signal. The disturbance is rejected by both controllers with a KC settling time $t_{sKC}=9$ s and a ZN settling time $t_{sZN}=20$ s. The disturbance is removed at $t=33$ s and the process returns to its reference position in $t_{sKC}=10$ s and $t_{sZN} =25$ s, respectively.

The experimental disturbance rejection test proves once more the efficacy of the KC controller when compared to the ZN.

Both experiments show that the closed loop system with the KC controllers obtains an improvement of more than 50% for the settling time of every tackled scenario.

VI. CONCLUSION

The paper presents the experimental validation of a novel autotuning method called the KC autotuner. The procedure uses a single sinusoidal test to determine the process' imaginary and real parts at the chosen frequency.

Two PID controllers are tuned using the KC tuning method and the ZN approach with the purpose of reference tracking and disturbance rejection of a VTOL experimental setup. The controllers are validated through multiple experimental tests. The PID controller tuned using the KC method proved superior to the controller tuned by ZN for every test case.

ACKNOWLEDGEMENT

This work was supported by a mobility grant of the Romanian Ministry of Research and Innovation, CNCS - UEFISCDI, project number PN-III-P1-1.1-MC-2019-0420, within PNCDI III.

REFERENCES

- [1] K. J. Astrom and T. Hagglund, "Automatic tuning of simple regulators with specifications on phase and amplitude margins," *Automatica*, vol. 20, no. 5, pp. 645–651, 1984.
- [2] K. J. Astrom, T. Hagglund, C. Hang, and W. Ho, "Automatic tuning and adaptation for PID controllers—A survey," *IFAC Proceedings Volumes*, vol. 25, no. 14, pp. 371–376, 1992.
- [3] S. H. Shen and C. C. Yu, "Use of relay-feedback test for automatic tuning of multivariable systems," *AIChE Journal*, vol. 40, no. 4, pp. 627–646, 1994.
- [4] Y. G. Wang, Z. G. Shi, and W. J. Cai, "PID auto-tuner and its application in HVAC systems," presented at the American Control Conference, 2001.
- [5] I. Birs, D. Copot, C. I. Muresan, R. De Keyser, and C. M. Ionescu, "Robust fractional order PI control for cardiac output stabilisation," *IFAC-PapersOnLine*, vol. 52, no. 1, pp. 994–999, 2019.
- [6] J. Berner, K. J. Astrom, and T. Hagglund, "Towards a new generation of relay autotuners," *IFAC Proceedings Volumes*, vol. 47, no. 3, pp. 11288–11293, 2014.
- [7] I. Nascu, R. D. Keyser, S. Folea, and T. Buzdugan, "Development and evaluation of a PID auto-tuning controller," in *Proc. IEEE International Conference on Automation, Quality and Testing, Robotics*, 2006.
- [8] M. Gregoire, A. Desbiens, and E. Richard, "Development of an auto-tuning PID and applications to the pulp and paper industry," presented at Third International Conference on Industrial Automation, 1999.
- [9] Y. Lim, R. Venugopal, and A. G. Ulsoy, "Auto-tuning and adaptive control of sheet metal forming," *Control Engineering Practice*, vol. 20, no. 2, pp. 156–164, 2012.
- [10] M. Cetin and S. Iplikci, "A novel auto-tuning PID control mechanism for nonlinear systems," *ISA Transactions*, vol. 58, pp. 292–308, Sep. 2015.
- [11] H. P. Huang and C. C. Chen, "Autotuning of PID controllers for second order unstable process having dead time," *Journal of Chemical Engineering of Japan*, vol. 32, no. 4, pp. 486–497, 1999.
- [12] H. Rasmussen, *Automatic Tuning of PID Regulators*, Aalborg University, Dept. of Control Engineering, 2002.
- [13] J. G. Ziegler and N. B. Nichols, "Optimum settings for automatic controllers," *Journal of Dynamic Systems, Measurement, and Control*, vol. 115, pp. 220–222, Jun. 1993.
- [14] C. C. Hang, K. J. Astrom, and Q. G. Wang, "Relay feedback auto-tuning of process controllers—A tutorial review," *Journal of Process Control*, vol. 12, no. 1, pp. 143–162, 2002.
- [15] Y. Zhang, L. Zhang, and Z. Dong, "An MEA-tuning method for design of the PID controller," *Mathematical Problems in Engineering*, vol. 2019, 2019.
- [16] R. De Keyser, C. I. Muresan, and C. M. Ionescu, "Universal direct tuner for loop control in industry," *IEEE Access*, vol. 7, pp. 81308–81320, 2019.
- [17] J. Berner, K. Soltesz, T. Häggglund, and K. Åström, "An experimental comparison of PID autotuners," *Control Engineering Practice*, vol. 73, pp. 124–133, April 2018.
- [18] R. De Keyser, C. Muresan, and C. Ionescu, "A novel auto-tuning method for fractional order PI/PD controllers," *ISA Transactions*, vol. 62, pp. 268–275, May 2016.
- [19] F. Hassan, A. C. Zolotas, and T. Smith, "Optimized Ziegler-Nichols based PID control design for tilt suspensions," *Journal of Engineering Science and Technology Review*, vol. 10, no. 5, pp. 17–24, 2017.

Robin De Keyser received the M.Sc. degree in electromechanical engineering and the Ph.D. degree in control engineering from Ghent University, Ghent, Belgium, in 1974 and 1980, respectively. He is currently emeritus professor of control engineering with the Faculty of Engineering, Ghent University. He is author/co-author of approximately 500 publications in journals, books, and conference proceedings. He acted as an External Review Expert for several European Commission research programs and is one of the pioneers who produced the original concepts of predictive control during the 1980s. His teaching and research activities include model predictive control, autotuning and adaptive control, modeling and simulation, and system identification. His research interests are application-driven with many pilot implementations in technical and nontechnical systems, including chemical, steel, marine, mechatronic, semiconductor, power electronics, and biomedical systems.

Isabela Birs is a Ph.D. student at the Technical University of Cluj-Napoca, Romania and at Ghent University, Belgium. Her interests are related to the application of fractional-order calculus, vibration suppression and the nanomedical field.

Cristina Muresan received the degree in control systems in 2007, and the Ph.D. in 2011 from Technical University of Cluj-Napoca, Romania. She is currently associate professor at the Technical University of Cluj-Napoca, Automation Department, Romania. Since 2007, she has published over 100 papers and book chapters, amongst which 2 have been awarded by the Romanian government. She has been and currently is involved in more than 10 research grants, all dealing with multivariable and fractional order control. Her research interests include modern control strategies, such as predictive algorithms, robust nonlinear control, fractional order control, time delay compensation methods and multivariable systems.